Published in final edited form as:
Toxicol Sci. 2017 October 01; 159(2): 354–365. doi:10.1093/toxsci/kfx146.

Metabolic disruption early in life is associated with latent carcinogenic activity of dichloroacetic acid in mice

Leah C. Wehmas[*], **Anthony B. DeAngelo**[*], **Susan D. Hester**[*], **Brian N. Chorley**[*], **Gleta Carswell**[*], **Greg R. Olson**[†], **Michael H. George**[*], **Julia H. Carter**[‡], **Sandra R. Eldridge**[‖,¶], **Anna Fisher**[*], **Beena Vallanat**[*], and **Charles E. Wood**[*,§]

[*]National Health and Environmental Effects Research Laboratory, U.S. Environmental Protection Agency, Research Triangle Park, NC, USA;

[†]Toxicologic Pathology Associates, Jefferson, AK, USA;

[‡]Wood Hudson Cancer Research Laboratory, Newport, KY, USA;

[‖]Pathology Associates International, Durham, NC, USA;

Abstract

Early-life environmental factors can influence later-life susceptibility to cancer. Recent evidence suggests that metabolic pathways may mediate this type of latency effect. Previously we reported that short-term exposure to dichloroacetic acid (DCA) increased liver cancer in mice 84 weeks after exposure was stopped. Here we evaluated time course dynamics for key events related to this effect. This study followed a stop-exposure design in which 28-day-old male B6C3F1 mice were given the following treatments in drinking water for up to 93 weeks: deionized water (dH_2O, control); 3.5 g/l DCA continuously; or 3.5 g/l DCA for 4–52 weeks followed by dH_2O. Effects were evaluated at eight interim time points. A short-term biomarker study was used to evaluate DCA effects at 6, 15, and 30 days. Liver tumor incidence was higher in all DCA treatment groups, including carcinomas in 82% of mice previously treated with DCA for only 4 weeks. Direct effects of DCA in the short-term study included decreased liver cell proliferation and marked mRNA changes related to mitochondrial dysfunction and altered cell metabolism. However, all observed short-term effects of DCA were ultimately reversible, and prior DCA treatment did not affect liver cell proliferation, apoptosis, necrosis, or DNA sequence variants with age. Key

[§]To whom correspondence should be addressed: Charles E. Wood, U.S. Environmental, Protection Agency, B105-03, 109 T.W. Alexander Drive, Research Triangle Park, NC 27711, USA, Tel: +1 919 541 1171; Fax: +1 919 541 0694; wood.charles@epa.gov.
[¶]Present address: Developmental Therapeutics Program, Division of Cancer Treatment and Diagnosis, National Cancer Institute, Rockville, MD, USA

Author Contributions

Author contributions include the following: C.E.W. and A.B.D. organized the study; C.E.W. wrote the manuscript; A.B.D. and M.G. designed the animal experiment and coordinated generation of in-life and pathology data; G.R.O. served as primary study pathologist; L.C.W., S.D.H., G.C., and B.N.C. generated and analyzed gene expression data; J.H.C. generated apoptosis data; S.R.E. generated cell proliferation data; A.F., B.V., S.D.H., B.N.C., and C.E.W. generated and analyzed amplicon data; and L.C.W., S.D.H., and B.N.C. helped to draft the manuscript. All authors read and approved the final report.

Disclosures

The research described in this article has been reviewed by the EPA and approved for publication. Approval does not signify that the contents necessarily reflect the views and the policies of the Agency. Mention of trade names or commercial products does not constitute endorsement or recommendation for use. Contractor roles did not include establishing Agency policy.

Conflict of Interest Statement: None declared.

intermediate events resulting from transient DCA exposure do not fit classical cytotoxic, mitogenic, or genotoxic modes of action for carcinogenesis, suggesting a distinct mechanism associated with early-life metabolic disruption.

Keywords

carcinogenesis; metabolism; early-life exposure; liver; dichloroacetic acid

Introduction

Cancer is now recognized as a life-stage disease. While the vast majority of human cancers are associated with increased age (Siegel *et al.* 2016), the genetic and epigenetic processes that drive and ultimately characterize malignancy often begin much earlier in life (Anisimov 2007; Balducci and Ershler 2005; Kuppusamy *et al.* 2015). Environmental factors may accelerate these processes and thereby alter risk years after an original exposure or event. For chemical carcinogens, we now know from both experimental and epidemiologic studies that changes initiated early in life can increase future susceptibility to cancer (Ginsberg 2003; Grandjean *et al.* 2015; Mahabir *et al.* 2012; Hoover *et al.* 2011; Smith *et al.* 2006; Weinhouse *et al.* 2014), often beyond that seen with adult-only exposure, and that the scope of these latent effects extends well beyond direct mutagenic agents (EPA 2005a; Barton *et al.* 2005; Halmes *et al.* 2000; Boekelheide *et al.* 2012). This evidence has highlighted the need for biomarkers that are persistently altered following exposure to a potential carcinogen and clearly associated with risk later in life.

In 2005, the U.S. Environmental Protection Agency (EPA) issued a guidance addressing general issues and susceptibility factors related to early-life exposure to carcinogens (EPA 2005a). This document defined specific life-stage adjustments for carcinogenic potency, called age-dependent adjustment factors (ADAFs), but only for chemicals with a primary mutagenic mode of action (MOA). For carcinogens acting through a non-mutagenic MOA, or those in which the MOA is unknown, standard methods of quantitative risk assessment were recommended (*i.e.*, without ADAFs) (EPA 2005b). This distinction was based on a lack of sufficient information to determine general adjustments for non-mutagenic agents with latent carcinogenic effects. The guidance further noted that as new MOA information and methods for quantifying early-life risk estimates become available, ADAF recommendations would be updated to include pathways other than mutagenicity. The current case study was developed to support this effort and examine non87 genetic effects that may persist and mediate health outcomes later in life.

The reference chemical for this study was dichloroacetic acid (dichloroacetate, DCA), which was widely studied in the 1990s as a disinfection by-product of drinking water chlorination (EPA 2003). Biochemically, DCA is similar to pyruvate and thus affects many fundamental pathways of cellular metabolism. Some of these effects may persist over time, which has led to the characterization of DCA as a metabolic reprogramming agent (*e.g.*, Phan *et al.* 2014; Zhang and Yang 2013). Previously, we showed that early-life postnatal exposure to DCA for 10 weeks increased the incidence of liver cancer in male and female mice 84 weeks after

exposure was stopped (Wood *et al*. 2015b), capturing the majority of carcinogenic effect reported previously after ≥90 weeks of continuous exposure (DeAngelo *et al*. 1991). However, there was no clear evidence of a persistent molecular footprint of DCA at weeks of age. The primary goal of the current study was to investigate key drivers of this effect by mapping time course changes following early-life DCA exposure.

DCA disrupts cell metabolism through several different pathways. One of the most widely studied effects is inhibition of pyruvate dehydrogenase kinase (PDK). Decreased PDK activity facilitates oxidative metabolism by increasing pyruvate dehydrogenase (PDH) activity, reducing glycolysis, and shunting glucose into the mitochondria (EPA 2003; Bonnet *et al*. 2007; Stacpoole *et al*. 2008; Zhang *et al*. 2016). DCA can also irreversibly inhibit glutathione S-transferase zeta 1 (GSTZ1) (Tseng *et al*. 2000), an enzyme that helps protect cells against oxidative stress (Blackburn *et al*. 2006). In the liver, DCA induces rapid accumulation of glycogen, resulting in cytoplasmic vacuolation and potential cell death of hepatocytes (Kato-Weinstein *et al*. 1998; DeAngelo *et al*. 1999). Collectively, these effects may result in chronic oxidative stress, cytotoxicity, regenerative proliferation, secondary DNA damage, and cancer. For this study, we hypothesized that metabolic changes following DCA exposure would persist over time, leading to increased oxidative stress and cell injury with age.

Methods

Study design

This experiment followed a stop-exposure design in which male B6C3F1 mice (n=404) were divided into the following treatment groups: deionized water (dH_2O, control); 3.5 g/l DCA continuously; or 3.5 g/l DCA for 4, 10, 26, or 52 weeks followed by dH_2O for up to 93 weeks. Groups are designated by DCA and dH_2O treatment times separated by a vertical bar (*e.g.*, 10|83 indicates 10 weeks of DCA followed by dH2O for up to 83 weeks). Animals were humanely euthanized by CO_2 at study end for all groups and at eight interim time points (10, 15, 26, 31, 52, 57, and 78 weeks of treatment) for a subset of groups (Figure 1A). Interim time points were selected to evaluate DCA carryover effects near-term (5 weeks) and longer-term (≥16 weeks). Liver samples were collected from all groups at all time points. A targeted short-term study was also conducted to investigate early dose-related effects of DCA on liver gene expression, cell proliferation, and apoptosis. For the latter study, male B6C3F1 mice (n=120) were randomized by weight to receive dH_2O alone or with DCA added at 0.5, 1.0, 2.0, and 3.5 g/l (n=8/group) for 6, 15, or 30 days (Figure 1B).

All animals were observed daily for clinical signs of toxicity and monitored regularly for water intake and body weight (BW). Mice were obtained at 21 days of age from Charles River Laboratories (CRL) (Morrisville, NC), acclimated for 7 days before treatment, housed in laminar flow rooms in polycarbonate cage, maintained under standard conditions (20±2 C °; 40–60% relative humidity; 12hr light/dark cycle), and fed *ad libitum* Purina 5001 laboratory rodent diet (Purina Test Diets, St. Louis, MO) in an AAALAC International-accredited animal facility at the U.S. EPA. An Institutional Animal Care and Use Committee approved all procedures involving animal use.

Drinking water dosing

DCA (CAS 79–43-6, Aldrich, Milwaukee, WI) was administered in drinking water as previously reported (Wood *et al.* 2015a; DeAngelo *et al.* 1999). Doses for chronic and short-term studies were selected based on prior carcinogenicity findings in male mice following long-term (DeAngelo *et al.* 1999) and transient (Wood *et al.* 2015a) exposures. The target 3.5 g/l dose in mice (429 mg/kg/d) was equivalent to 65 mg/kg/d in humans based on a scaling factor of $BW^{0.75}$ (EPA 2003). This dose is up to ~10^5 times greater than DCA concentrations measured in finished drinking water samples (33 to 160 μg/l) (EPA 2003) and ~2.6 times greater than doses used clinically in studies of children and adolescents with congenital metabolic diseases (12.5 mg/kg every 12 hours) (*e.g.*, Stacpoole *et al.* 2008).

Actual DCA doses were estimated based on mean water intake, BW, and water DCA concentrations (DeAngelo et al. 1999). Daily water consumption (ml/kg/day) by cage was measured every 4–5 weeks from weeks 4–89 in the chronic study and weekly in the short-term study. Water pH was adjusted to 6.8–7.2 using NaOH. Water solutions were stored at 4–6°C, changed every 5–7 days, and sampled and analyzed throughout both studies. Stock drinking water samples were prepared every 12–14 days and analyzed by ultraviolet absorption at 231 nm with a Beckman DU Series 600 spectrophotometer (Beckman Coulter, Brea, CA) to confirm DCA concentration. Prior studies have shown DCA to be stable over a 1- to 2-week period (DeAngelo et al. 1996; DeAngelo et al. 1999; Herren-Freund et al. 1987).

Overall water consumption in the chronic study was 5–22% lower in DCA groups compared to controls (Supplementary Table S1). This effect was more pronounced at earlier time points and quickly rebounded after DCA was stopped (Supplementary Figure S1). By week 52, water intake was 100–125 ml/kg/d in all groups. In the short-term study, DCA showed a dose-related effect at 6, 15, and 30 days (33–39% lower intake at high dose) (Supplementary Table S2).`

Liver histology and pathology

Necropsy procedures were conducted by pathology staff at CRL/Pathology Associates International (PAI; Research Triangle Park, NC). Livers were grossly examined, weighed, fixed, trimmed, and processed into paraffin blocks. A portion of each liver (multiple lobes, mixed) was frozen for RNA and DNA analyses. Fixed tissues were placed in 10% buffered formalin and transferred to 70% ethanol after 18–24 hours. In the chronic study, embedded tissues were sectioned at 5–6 μm onto glass slides and stained with hematoxylin and eosin (H&E) using standard procedures. Four sections of liver (two each from grossly normal portions of left and median lobes) were evaluated via light microscopy by a certified pathologist (GRO). Mass lesions were counted, collected, sectioned, and examined separately. Histopathologic examination of liver tissues used standard criteria and nomenclature for neoplastic and non-neoplastic lesions. Where applicable, lesion severity was scored using a qualitative 0–4 scale (0=absent, 1=minimal, 2=mild, 3=moderate, 4=severe).

Cell proliferation and apoptosis

Liver cell proliferation was determined by immunohistochemical (IHC) staining for proliferating cell nuclear antigen (PCNA) and 5-bromo-2'-deoxyuridine (BrdU). Apoptosis was evaluated by TdT-mediated dUTP nick end labeling (TUNEL). In the chronic study, labeling indices (LI) were measured at all interim timepoints for PCNA and week 57 for TUNEL. In the short-term study, LIs were measured at 6, 15, and 30 days for BrdU and 30 days for TUNEL. IHC staining was performed at PAI using established methods (Eldridge *et al.* 1996). PCNA IHC included the PC10 monoclonal antibody (Dako Corp., Carpinteria, CA), avidin-biotin peroxidase method for secondary labeling (Vectastain ABC kit, Vector Labs, Burlingame, CA), and 3,3'-diaminobenzidine (DAB) as the chromogen (Sigma Chemical Co., St. Louis, MO). For the short-term study, mice were implanted with subcutaneous osmotic pumps (Alzet Model 2001, 1 ml/hr, ALZA Corp., Palo Alto, CA) containing 2.4 mg/ml BrdU (CAS 59–14-3) in phosphate-buffered saline (pH 6.8–7.2) 5 days before each scheduled sacrifice. BrdU labeling used the MAS 250c monoclonal antibody (Accurate Chemical and Scientific Corp., Westbury, NY), streptavidin conjugated to horseradish peroxidase as label, and DAB as chromogen (Eldridge *et al.* 1996). TUNEL staining was performed at Wood Hudson Cancer Research Laboratory (Newport, KY) as described previously (Gavrieli *et al.* 1992; Snyder *et al.* 1995) using pre-treatment of slides with protease K (Sigma Chemical Co.) and staining with Tdt and biotinylated dUTP. Sections of mouse duodenum, epidermis, and post-irradiation prostate were run as positive controls for BrdU, PCNA, and TUNEL staining, respectively. Non-immune rabbit serum applied at the same concentrations as the primary antibodies served as a negative control for non-specific BrdU or PCNA staining (none observed).

To quantify cell proliferation and apoptosis, slides were coded and cells in at least 10 randomly selected fields from the left liver lobe (excluding proliferative lesions) were visually counted (+/−) via light microscopy at 40x objective by an observer blinded to treatment groups. BrdU and PCNA staining was nuclear, while TUNEL staining was nuclear and/or cytoplasmic. A minimum of 2000 cells/section were counted and used to calculate a LI of %-positive cells. Minimum counts were based on previous estimates of background Lis in the B6C3F1 mouse liver (*e.g.*, Eldridge *et al.* 1993; Snyder *et al.* 1995). BrdU and PCNA staining was quantified at PAI, while TUNEL staining was quantified at Macro Micro Photoillustrations (Covington, KY).

Serum ALT

Blood was collected at necropsy and processed to serum. Serum alanine aminotransferase (ALT) was measured as an indicator of liver cytotoxicity with a Beckman DU Series 600 spectrophotometer using routine methods and standard kits (Sigma Chemical Co.).

Nucleic acid isolation

For gene expression analysis, total liver RNA was isolated from frozen liver (~20 mg/sample) homogenized in RNAzol®RT (Molecular Research Center, Cincinnati, OH) with a Precellys® 24 homogenizer (Bertin Technologies, Villeurbanne, France). DNA was removed via 4-bromoanisole phase separation followed by alcohol precipitation and wash. RNA was purified with the RNeasy MinElute column protocol (Qiagen GmbH, Hilden, Germany).

RNA integrity was evaluated using an Agilent 2100 Bioanalyzer (Agilent Technologies, Palo Alto, CA) and quantified using a Qubit fluorometer (ThermoFisher Scientific, Waltham, MA). DNA was isolated from frozen liver (~25 mg/sample) following bead homogenization, as described for total RNA. Homogenates were centrifuged and then incubated for 1hr at 56°C with 40µl of proteinase K (50 µg/µl stock) in a Vortemp mixer at low rpm. Lysates were purified using a QIAmp kit protocol (Qiagen GmbH) and precipitated with ethanol. DNA concentrations were determined using a NanoDrop ND-1000 spectrophotometer (NanoDrop Technologies, Wilmington, DE).

RNA-sequencing

A subset of 24 frozen liver samples from the short-term study were arbitrarily selected from the 0, 1.0, 2.0, and 3.5 g/l DCA groups at 6 days (n=6/group) and used for whole genome RNA-sequencing (RNA-seq). Sequencing was performed at Expression Analysis (EA; Q2 Solutions - Quintiles, Durham, NC) as described previously (Hester *et al.* 2016). cDNA libraries were generated from total RNA using the TruSeq Stranded Total RNA with RiboZero Gold Sample Prep Kit (Illumina, San Diego, CA). Final libraries were analyzed using an Agilent 2100 Bioanalyzer (DNA 1000 kit), quantitated by reverse-transcription polymerase chain reaction (RT-qPCR) (KAPA Library Quant Kit, KAPA Biosystems), barcode-labeled, and sequenced on an Illumina HiSeq 2500 instrument with 2×50bp-paired end flow cells. Complete RNA-seq FASTQ datasets are available through the NCBI Gene Expression Omnibus (GEO) (www.ncbi.nlm.nih.gov/geo/) (accession# GSE86065).

RNA-seq data were analyzed as described previously (Hester *et al.* 2016). Basecall files were converted into FASTQ format (CASAVA v. 1.8.2) and demultiplexed. Adapters and low-quality bases (Q-score <7) on read ends were trimmed. Reads with any one base at ≥95% frequency, >4 Ns in a row, average quality score <25 or length < 25 nucleotides after trimming were removed using RNAv9 pipeline (EA, Q2 Solutions, Durham, NC) (https://github.com/ExpressionAnalysis/ea-utils/). Quality-filtered reads were aligned to External RNA Controls Consortium (ERCC), Illumina and PhiX spike-ins, and off-target biological material sequences to evaluate library construction, sequencing, and potential DNA contamination. To quantify transcripts, clipped FASTQ files were aligned to the reference mouse genome (*Mus musculus*-GRCm38/mm10) and transcriptome (RefSeq transcript 2015–02-02) in Partek Flow® (Build v4.0.16.0128, St. Louis, MO). Gene counts were quantified using the Partek® expectation maximization algorithm (Partek E/M) (Li and Dewey 2011) and normalized to reads per kilobase of transcript per million mapped reads (RPKM) with a 0 count offset of 1. Results were then filtered to remove genes with maximum expression <1 across all samples. Differential gene expression analysis was performed on filtered, normalized RNA-seq counts with Partek® Gene-Specific Analysis. This analysis uses transcript-specific data to identify the best response distribution (Normal, Lognormal with shrinkage, and Negative Binomial models) using (a) Akaike information criterion corrected for small sample size and (b) F-statistics and a false discovery rate (FDR) filter of 5% to identify significant differentially expressed genes (DEGs) between DCA treatment groups relative to control. Analyses of DEGs were conducted in Ingenuity Pathway Analysis (IPA) Knowledgebase (Qiagen) using tools for canonical pathway

identification and upstream regulator analysis (http://pages.ingenuity.com/rs/ingenuity/images/0812%20upstream_regulator_analysis_whitepaper.pdf).

Target mRNA expression

Sequencing results from the short-term study were used to identify candidate genes that may be persistently altered in the long-term study. mRNA expression was measured using RT-qPCR in control and 3.5 g/l DCA groups at 6 days (acute); 10-week DCA stop-exposure groups at 10, 26, 52, 78, and 93 weeks (time course); control, 26-week, 52-week, and continuous DCA exposure groups at 78 weeks (long-term carry-over); and continuous DCA exposure group at 93 weeks (age control). Nine target mRNAs were analyzed including metabolic genes highly induced in a dose-dependent manner at 6 days. Reference genes (*Tbp, Rplp0, Rps18*, and *Ywhaz*) were selected from a standard normalization panel based on RNA-seq data. Primers and probes were designed using the SYBR® Green PrimePCR™ platform (Bio-Rad, Hercules, CA), and cDNA was generated using iScript Reverse Transcription Supermix. RT-qPCR reactions were prepared using Bio-Rad SsoAdvanced Universal SYBR Green Supermix and run in duplicate on a Bio-Rad CFX384 instrument. Differences in gene expression were quantified using the Pfaffl method (ratio = $(E_{target})^{\Delta cq,\ target\ (calibrator - test)}/(E_{ref})^{\Delta cq,\ ref\ (calibrator - test)}$) (Pfaffl 2001) and normalized by geometric averaging of multiple internal control genes for relative quantification (Vandesompele et al. 2002).

DNA amplicon resequencing

DNA sequence variants were evaluated using the Illumina TruSeq amplicon platform for targeted resequencing (Wood *et al.* 2015a). Liver DNA was analyzed from a total of 42 mice in the following groups from the chronic study: control (26, 78, and 93 weeks); 10-week DCA (10, 26, 52, 78, and 93 weeks); 26-week DCA (26 and 78 weeks); and 78-week DCA (78 weeks) (n=3–4/group). Amplicons for target genes were adapted from the human TruSeq Amplicon Cancer Panel (n=38) or identified from the literature as having an association with liver cancer (n=27) (Wood *et al.* 2015a). Mouse orthologs were generated using Illumina DesignStudio Software using the *Mus musculus* UCSC NCBI37/mm9 reference genome. Amplicons were designed within exonic or 3'/5' UTRs using the Sanger Cosmic database (http://cancer.sanger.ac.uk/cancergenome/projects/cosmic/). Target regions were focused on sites of high mutational activity. Oligonucleotide DNA templates consisting of target and universal primer regions were generated, PCR-amplified using indexed primers, pooled, and sequenced on an Illumina MiSeq instrument. Acceptable amplicons corresponded to 472 target regions across 62 different genes. All samples were sequenced in duplicate using standard Illumina reagents and protocols.

Amplicon data were generated in variant call format (.vcf) using Illumina MiSeq Reporter. Overall coverage was 104x with an average of 131k clusters passing filter (PF) per sample. "Raw" variant calls (VCs) were identified based on differences with the mm9 reference sequence and quality-filtered using predefined Illumina exclusion criteria, including variant frequency (VF) <1%, genotype quality <30, IndelRepeatLength >8, low coverage (no genotype called), and high variant strand bias. A total of 11,326 VCs passed initial quality filters (n=5568 and n=5758 in "a" and "b" sample replicates, respectively). There was 92%

concordance in total VCs PF and 79% overlap in exact VCs PF between replicates. Called variants were then examined in reference to parental strains for B6C3F1 hybrid mice. Briefly, mm9 coordinates for all VC loci (n=117) were converted to mm10 coordinates using the UCSC liftOver tool (https://genome.ucsc.edu/util.html) and screened for heterozygosity using the Sanger Institute reference genomes for C57BL/6NJ and C3H/HeJ strains (http://www.sanger.ac.uk/science/data/mouse-genomes-project).

Other statistical analyses

In-life and histopathology data were analyzed using SAS statistical package v9.4 (SAS Institute, Cary, NC) and Graphpad Software (http://graphpad.com/quickcalcs/contingency1.cfm). Early mortality was evaluated using the LIFETEST procedure to generate Kaplan-Meier survival distributions, followed by pairwise testing of homogeneity between survival curves. A two-sided Fisher's Exact Test was used to evaluate group differences in liver lesion incidence and final variant number. Continuous data were screened for normality and homogeneity of variance. Analysis of variance (ANOVA) was used to determine group differences for continuous data meeting these criteria. For non-parametric data, group differences were evaluated using a Kruskal-Wallis ANOVA followed by Wilcoxon rank sum pairwise tests. For the short-term study, a Jonckheere test was used to evaluate dose trends in LI data. Pairwise comparisons included treatment groups at each time point *versus* the respective control group. A Bonferroni multiple-comparison correction was applied to all related pairwise and trend test *P-values*. Continuous data are reported as mean ± standard error unless otherwise stated.

Results

Early-life DCA exposure did not increase mortality

Mortality incidence and survival curves in the chronic study are shown in Supplementary Table S1 and Supplementary Figure S2, respectively. A Univariate Chi-Squares for the Log-Rank Test showed no significant association between overall mortality and liver tumor incidence. Similarly, pairwise testing of homogeneity between survival curves showed no significant differences between the dH_2O control group and DCA treatment groups.

DCA reduced body weight with variable recovery times

Continuous DCA treatment in the chronic study resulted in progressively lower BW with 345 increased duration of exposure compared to dH_2O controls, from −5% at 10 weeks to −20% at 93 weeks (Supplementary Figures S3 and S4). Upon withdrawal of DCA, BW recovered to control levels in all groups (prior to 93 weeks) (Supplementary Table S3). Recovery times for terminal BW varied from <5 weeks (52-week DCA) to >21 weeks (10-week DCA) (Supplementary Figures S3 and S4).

Transient DCA exposure increased cancer incidence in all treatment groups

Both incidence and number of hepatocellular (HC) carcinomas and combined HC adenomas/carcinomas were higher in all DCA treatment groups ($P < 0.05$ compared to dH_2O controls) (Table 1; Supplementary Table S4). Continuous DCA treatment resulted in the highest incidence of HC carcinomas (93% at ≥52 weeks). Prior treatment with DCA for only 4

weeks captured most of this effect (82% incidence at ≥52 weeks). At 93 weeks of treatment, there were no statistically significant differences in the incidence of combined HC adenomas/carcinomas between any of the DCA treatment groups ($P > 0.1$ for all) (Supplementary Table S4). However, longer duration of DCA exposure did result in a greater number of HC tumors at ≥52 weeks (>2-fold higher tumors per animal in the 93-week DCA group compared to all other groups) (Table 1) and higher incidence of tumors at interim time points (Supplementary Table S4). At the 57- and 78-week time points (combined), groups exposed to DCA for ≥52 weeks had significantly higher HC tumor incidence compared to the 10- and 26-week DCA exposure groups ($P < 0.05$ for all) (incidence = 18%, 39%, 53%, 95%, and 100% for dH2O control, 10-, 26-, 52-, and 93-week DCA groups, respectively) (Figure 2A; Supplementary Table S4).

DCA induced transient effects on liver weight, hypertrophy, and cytotoxicity

In the long-term study, continuous treatment with DCA increased relative liver weights at 10, 26, and 52 weeks (Supplementary Table S3). Increased weights persisted beyond 5 weeks but eventually returned to control levels in all stop-exposure groups. For example, in the 10-week DCA exposure group liver weights returned to control levels by 31 weeks of treatment (Figure 2B). Weights then increased again later in the study, presumably due to expansion of proliferative lesions.

The most prominent non-neoplastic effect of direct DCA exposure was moderate to severe HC hypertrophy (cytomegaly), observed at all time points in the long-term study (Supplementary Table S6; Figure 2C). This change was associated with marked cytoplasmic vacuolization; minimal to mild pigmentation, likely due to cholestasis secondary to the marked HC hypertrophy; and minimal to mild HC necrosis (Supplementary Table S6; Figure 2C). DCA effects on HC hypertrophy generally tracked liver weight and resolved sometime after 5 weeks of recovery (Figure 2D), while HC necrosis resolved within 5 weeks of discontinuing DCA treatment in all stop-treatment groups (Figure 2E). All of these morphologic effects had resolved by 31 weeks for the 10-week DCA group, by 57 weeks for the 26-week DCA group, and by 78 weeks for the 52-week DCA group.

DCA increased foci but decreased short-term liver cell proliferation

The overall incidence of proliferative HC foci was higher in DCA stop-exposure groups (13–27%) compared to controls (5%) at ≥31 weeks (Supplementary Table S7). The 26-week (basophilic foci only) and 52-week (all foci and basophilic foci) DCA exposure groups had statistically significant increases compared to controls (Figure 3A). However, this effect was not associated with sustained induction of cell proliferation in the liver. The PCNA LI was generally low (<1.0%) across all treatment groups compared to proliferative lesions (foci and tumors), which had a mean LI of 5.9 ± 0.8%. Direct DCA treatment resulted in significantly higher PCNA LI at 10 weeks (0.3% vs. 0.1% in controls, $P < 0.05$) but not at other interim time points (Supplementary Table S8; Figure 3B). Prior DCA treatment did not result in significantly greater PCNA LI in any group at any time point (Figure 3B), and direct or prior DCA exposure did not significantly alter TUNEL LI at 57 weeks (Supplementary Table S8).

In the short-term dose-range study, direct DCA treatment increased absolute and relative liver weight in a dose-dependent manner starting at 6 days (Supplementary Table S5; Figure 3C) but did not induce a corresponding mitogenic effect. Rather, cell proliferation determined by BrdU LI was significantly lower in the 2.0 g/l and 3.5 g/l DCA groups at 6 and 15 days (Supplementary Table S9; Figure 3C and 3D). No significant group differences were observed for TUNEL LI at 30 days (Supplementary Table S9).

DCA induced marked disruption of metabolic pathways

Acute transcriptomic changes were measured by RNA-seq after 6 days of DCA treatment. Sequencing quality metrics are available in Supplementary Table S10. DCA treatment resulted in 943, 5602, and 5678 DEGs in the 1.0, 2.0, and 3.5 g/l dose groups, respectively, and clear separation of dose groups on PCA (Figure 4A). General concordance in DEGs and target pathways was seen across DCA doses; for example, the 3.5 g/l dose captured 84% (738/943) and 73% (4079/5602) of DEGS in the 1.0 and 2.0 g/l dose groups, respectively (Figure 4B). Highly altered DEGs related to fatty acid degradation/metabolism, including known targets of peroxisome proliferator-activated receptor (PPAR) signaling (*e.g., Cyp4a* and *Acot series, Ehhadh, Scd1*) (up), protease inhibition (*e.g., Serpina1e, Mug1, Itih1*) (down), long-chain fatty acid synthesis (*Elovl3*) (down), and gluconeogenesis (*Ppargc1a, Ppard* and *Pck1*) (down). A full list of RPKM-normalized DEG counts is provided in Supplementary Table S11. The most highly ranked canonical pathways at the 3.5 g/l DCA dose were Mitochondrial Dysfunction, Oxidative Phosphorylation, and NRF2-mediated Oxidative Stress Response (Figure 4C, Supplementary Table S12). Highly represented gene families included mitochondrial complex NADH:ubiquinone oxidoreductase subunits (NDUFs), cytochrome c oxidases, heat shock proteins, and ATP synthases (Supplementary Table S13). Further analysis of upstream transcriptional regulators for DEGs identified PPARα and rapamycin-insensitive companion of mTOR (RICTOR) as the top-ranked activated and inhibited regulators, respectively, at both the 2.0 and 3.5 g/l doses of DCA (Supplementary Table S14). Collectively, these changes indicated marked dysregulation of oxidative metabolism in the mitochondria and altered lipid and glucose homeostasis centered on acetyl coenzyme A (Ac-CoA).

We next examined the persistence of select target genes over time in liver samples from the chronic stop-exposure study. mRNAs related to metabolic disruption that were strongly induced by acute exposure to DCA (*e.g., Cyp4a10* and *Cyp4a14*) all returned to control levels within 5 weeks of stopping DCA (Figure 4D, 4E; Supplementary Table S15). Two genes repressed by DCA, *Herpud1* and *Serpina1e*, remained lower after DCA exposure but were also lower in dH_2O control groups at 78 and 93 weeks, suggesting that the lower expression was due to age rather than prior DCA treatment.

DCA did not increase DNA sequence variants

Sequence variants in liver DNA were evaluated in 1348 target loci across 62 key cancer related genes using targeted resequencing. The goal was to evaluate time course effects of prior DCA treatment on DNA sequence variants. We predicted that variants would increase with age and that DCA treatment would amplify this effect. Qualify-filtered variants at >1% frequency were initially identified at 160 loci (Figure 5A; Supplementary Table S16).

Average frequency for initial VCs passing filter was consistent between replicates and across individual samples (47% overall) (Figure 5B). Heterozygosity between parental strains (corresponding to reference and variant bases) was identified for 84% (134/160) of variant loci covering 95% (4140/4354) of all filtered VCs (Figure 5C; Supplementary Table S16). All of these heterozygosity VCs were located at the exact base coordinate(s) except for one (GSTA1), which was identified at a locus 2 bases from the target site (likely coordinate error). In addition, 4% (191/4354) of filtered VCs were located at insertion, deletion, or start/end sites of nucleotide repeat sequences (*e.g.*, G > GA base variant called at break site of G > 7 A bases) and potentially a result of technical PCR error (Clarke *et al.* 2001). The remaining 23 VCs were considered actual base changes. Among these VCs, there were no apparent age-related effects and no effects of direct or prior DCA exposure (Figure 5D).

Discussion

Metabolic trajectories established early in life can affect health outcomes later in life, including cancer. Environmental determinants of these metabolic shifts are poorly understood. DCA is a structural analog of pyruvate with distinctive 458 effects on cellular metabolism and bioenergetics. Previously we demonstrated latent effects of DCA on liver carcinogenesis in mice (Wood *et al.* 2015a). Here we investigated time course patterns for key events driving this effect. Early adult exposure to DCA for only 4 weeks resulted in 82% incidence of liver carcinoma at 97 weeks of age, capturing 86% of the carcinogenic effect observed with continuous DCA exposure at the same dose. Short-term genomic profiles showed marked disruption of lipid and carbohydrate metabolism pathways centered on Ac-CoA, including mitochondrial dysfunction, oxidative phosphorylation, and oxidative stress response. No evidence of direct mitogenesis, mutagenesis, or persistent cytotoxicity was observed. Collectively, these findings demonstrate long-term carcinogenic effects associated with transient metabolic disruption early in life.

The direct effects of DCA persisted for varying lengths of time after stoppage of treatment. The most pronounced morphologic changes were increased liver weight, hepatocellular hypertrophy, and cytoplasmic vacuolation, which lasted up to 26 weeks after stopping DCA treatment. These effects have previously been attributed to glycogenosis (EPA 2003; Lingohr *et al.* 2002; Kato-Weinstein *et al.* 1998; Sanchez and Bull 1990), which may be part of a misguided “energy overload” response induced by the pyruvate-like structure of DCA. Interestingly, the short-term mRNA profiles observed here did not highlight pathways specifically related to glycogen metabolism, and it is unclear to what extent these morphologic changes reflected transcriptional effects of DCA. Other effects included minimal to mild hepatocellular necrosis, inflammation, and pigmentation, all of which resolved within 5 weeks of stopping DCA in all stop-treatment groups, indicating a lack of sustained (or recurrent) cytotoxicity. All morphological outcomes were thus washed out in each DCA stop-treatment group prior to onset of tumors, raising the question of what molecular changes may have persisted and driven this later effect.

Our first rule-out was increased cell proliferation, which is a central key event in most established non-genotoxic MOAs for chemical carcinogens (Wood *et al.* 2015b; Holsapple *et al.* 2006). Primary causes of increased cell proliferation are mitogenesis and sustained

cytotoxicity. Here, we found that short-term DCA exposure *decreased* cell proliferation in a dose-dependent manner under exposure conditions of previous chronic studies. This acute anti-proliferative effect is distinctive among known (non-mutagenic) chemical carcinogens. Longer-term direct exposure (≥10 weeks) resulted in modest increases in cell proliferation, likely in response to the mild hepatocellular necrosis. The impact of this regenerative effect on latent carcinogenicity, if any, is considered minor given that it was not consistent across DCA treatment groups (statistically significant only at 10 weeks) and did not persist. This response may have contributed to the higher tumor number and earlier tumor onset in groups exposed to DCA for longer durations (≥52 weeks), but it was not required for the latent carcinogenic effect to occur given that the clear carcinogenic effect seen after 4 weeks of DCA treatment in the chronic study did not correspond to increased cell proliferation at 6, 15, or 30 days in the short-term study. Thus, for the 4-week DCA group, there was no evidence of a proliferative effect at any point during the exposure window (based on short-term study) or after the exposure window (based on long-term study). Collectively, these findings strongly suggest that classical mitogenic or cytotoxic proliferation-mediated pathways are not primary drivers for the latent carcinogenicity of DCA.

Another rule-out was direct DNA damage or mutagenicity, which has been investigated previously as a potential MOA for DCA-induced carcinogenesis following chronic exposure (DeAngelo *et al*. 1991; DeAngelo *et al*. 1996; Leavitt *et al*. 1997). Several health authorities have concluded that DCA is acting primarily through non-genotoxic mechanisms, although a definitive MOA has not been established (EPA 2003; WHO 2000; IARC 2004), and select studies have reported evidence of mutagenic potential. For example, one experiment in male transgenic B6C3F1 mice harboring the bacterial lacI gene found a significant increase in mutant frequency in the liver after 60 weeks of DCA treatment at 3.5 g/l (but not after 4 or 10 weeks of treatment) (Leavitt *et al*. 1997). Here, we used amplicon resequencing to survey sites of high mutational activity across 62 oncogenes and tumor suppressor genes and found no effects of direct or prior DCA exposure. The consistent detection of strain-dependent heterozygous variants (at ~50% frequency) supports the accuracy of this platform. However, the low number of total variants and lack of time course effects suggest that the 1% variant frequency threshold for the assay is simply too high for reliable detection of age-related variants. These findings are also consistent with data from the previous stop-exposure study, which showed no effect of prior DCA on DNA variants at 98 weeks of age (Wood *et al*. 2015a).

The transcriptional effects of DCA were generally consistent with increased pyruvate load, PDH activity, and oxidative mitochondrial metabolism. Recent studies suggest that this metabolic shift may decrease cell proliferation in various cancer cell lines treated with DCA (*e.g*., De Preter *et al*. 2015). Our data indicate that acute anti-proliferative effects may also occur in normal liver cells *in vivo* (*i.e*., in the absence of an aerobic glycolytic phenotype). However, direct links between the metabolic and later carcinogenic effects are not clear at this point. Overall genomic responses to DCA at 6 days were overwhelming (>5500 DEGs for 3.5 g/l dose), which may have obscured primary targets. Growth factor signaling pathways such as insulin or signal transducers and activators of transcription 5 (STAT5) were not represented in top-ranked pathways, and we did not see clear targeted effects on genes related to GSTZ activity or apoptosis/cell survival. We did note strong induction by

DCA of many known PPARα targets, many of which were increased by >100-fold. Further work is needed to determine whether this pattern represents an actual PPARα-dependent effect, given that previous studies of DCA report inconsistent or weak induction of peroxisomal enzyme activity (*e.g.*, Corton 2008) and no short-term mitogenic effects (typical of PPARα-activating liver carcinogens) were observed, or simply a convergent pattern due to an overall increase in peroxisomal oxidation of fatty acids secondary to increased Ac-CoA.

Paradoxically, much of the recent interest in DCA has focused on its role as a cancer preventive agent, based primarily on its ability to decrease conversion of glucose to lactate. This metabolic shunt, which is mediated by inhibition of PDK and activation of PDH, effectively blocks the preferred route of glucose metabolism for many types of cancer cells, known as the Warburg effect (Sutendra *et al.* 2013; Vander Heiden *et al.* 2009; Gatenby and Gillies 2004). DCA has thus been used experimentally as an “anti-Warburg” agent that increases mitochondrial oxidative phosphorylation at the expense of lactate production. Glycolysis-derived pyruvate can also be used to generate cytosolic Ac-CoA (Shyh-Chang *et al.* 2015), which was a key node for many of the genomic targets altered by DCA at 6 days. A recent study (Moussaieff *et al.* 2015) showed that DCA, by redirecting pyruvate toward Ac- CoA, increased histone acetylation and increased pluripotency in embryonic stem cells. While there are important differences in reprogramming of somatic and embryonic cells, these findings point to potential interactions between Ac-CoA resulting from DCA and epigenetic regulation of cell differentiation.

In 2011, Hanahan and Weinberg (2011) highlighted dysregulation of energy metabolism as an emerging hallmark of cancer, based on the idea that neoplastic cells require fundamental changes in cellular bioenergetics to support their increased growth and energy demands. In this study, we examined the long-term carry-over effects of a classical metabolic disrupting chemical. Transient exposure to DCA for a relatively short duration resulted in clear carcinogenic effects approaching that seen with lifetime exposure. This latent effect was associated with dramatic acute changes in oxidative metabolism but not short-term mitogenesis, sustained cytotoxicity, or increased DNA variants. Key intermediate events thus did not fit the classical modes of action for chemical carcinogenesis. Additional studies are needed to examine whether early-life metabolic disruption by DCA alters oxidative DNA damage, bioenergetic profiles, and epigenetic changes such as DNA methylation later in life. More broadly, this work should inform efforts to identify predictive biomarkers and model chemical effects based on short-term exposures.

Supplementary Material

Refer to Web version on PubMed Central for supplementary material.

Acknowledgements

The authors would like to acknowledge the late Dr. Harry W. Carter for his work related to imaging and analysis of TUNEL slides. We also thank Glenda Moser and Wen-Hsin Tsai for technical assistance with BrdU study evaluations; Natalia Ryan for assistance with DNA preparation; staff at EA Genomic Services, Q2 Solutions, for RNA-seq data generation and processing; Dennis House, Woodrow Setzer, Judy Schmid, Steve Kilburn, Tanya

Moore, Steve Kilburn, Bernard Most, and William Ward for data management and statistical support; and Drs. Santhini Ramasamy and William Irwin for critical review of this manuscript.

Funding

This work was supported by the U.S. EPA Office of Research and Development.

Abbreviations

Ac	CoA acetyl coenzyme A
Ad	adenoma
ADAF	age-dependent adjustment factors
ANOVA	analysis of variance
BW	body weight
BrdU	5-bromo-2’-deoxyuridine
Ca	carcinoma
Con	control
CRL	Charles River Laboratories
DAB	3,3’-diaminobenzidine
DCA	dichloroacetic acid
DEGs	differentially expressed genes
dH_2O	deionized water
EA	Expression Analysis
EPA U.S.	Environmental Protection Agency
ERCC	External RNA Controls Consortium
FDR	false discovery rate
GSTZ1	glutathione S-transferase zeta 1
GEO	Gene Expression Omnibus
HC	hepatocellular
H&E	hematoxylin and eosin
IHC	immunohistochemistry
IPA	Ingenuity Pathway Analysis
LI	labeling index

mRNA	messenger ribonucleic acid
MOA	mode of action
NOS	not otherwise specified
PAI	Pathology Associates International
PCA	Principal component analysis
PNCA	proliferating cell nuclear antigen
PDH	pyruvate dehydrogenase
PDK	pyruvate dehydrogenase kinase
PF	passing filter
PPAR	peroxisome proliferator-activated receptor
RT-qPCR	reverse transcription quantitative polymerase chain reaction
RNA-seq	RNA-sequencing
RPKM	reads per kilobase of transcript per million mapped reads
rRNA	ribosomal RNA
TUNEL	TdT-mediated dUTP nick end labeling
VC	variant call
VF	variant frequency

References

Anisimov VN (2007). Biology of aging and cancer. Cancer Control 14, 23–31. [PubMed: 17242668]

Balducci L, and Ershler WB (2005). Cancer and ageing: a nexus at several levels. Nat Rev Cancer 5, 655–62. [PubMed: 16056261]

Barton HA, Cogliano VJ, Flowers L, Valcovic L, Setzer RW, and Woodruff TJ (2005). Assessing susceptibility from early-life exposure to carcinogens. Environ Health Perspect 113, 1125–33. [PubMed: 16140616]

Blackburn AC, Matthaei KI, Lim C, Taylor MC, Cappello JY, Hayes JD, Anders MW, and Board PG (2006). Deficiency of glutathione transferase zeta causes oxidative stress and activation of antioxidant response pathways. Mol Pharmacol 69, 650–7. [PubMed: 16278372]

Boekelheide K, Blumberg B, Chapin RE, Cote I, Graziano JH, Janesick A, Lane R, Lillycrop K, Myatt L, States JC, Thayer KA, Waalkes MP, and Rogers JM (2012). Predicting later-life outcomes of early-life exposures. Environ Health Perspect 120, 1353–61. [PubMed: 22672778]

Bonnet S, Archer SL, Allalunis-Turner J, Haromy A, Beaulieu C, Thompson R, Lee CT, Lopaschuk GD, Puttagunta L, Bonnet S, Harry G, Hashimoto K, Porter CJ, Andrade MA, Thebaud B, and Michelakis ED (2007). A mitochondria-K+ channel axis is suppressed in cancer and its normalization promotes apoptosis and inhibits cancer growth. Cancer Cell 11, 37–51. [PubMed: 17222789]

Clarke LA, Rebelo CS, Goncalves J, Boavida MG, and Jordan P (2001). PCR amplification introduces errors into mononucleotide and dinucleotide repeat sequences. Mol Pathol 54, 351–3. [PubMed: 11577179]

Corton JC (2008). Evaluation of the role of peroxisome proliferator-activated receptor alpha (PPARalpha) in mouse liver tumor induction by trichloroethylene and metabolites. Crit Rev Toxicol 38, 857–75. [PubMed: 18821149]

DeAngelo AB, Daniel FB, Stober JA, and Olson GR (1991). The carcinogenicity of dichloroacetic acid in the male B6C3F_1 mouse. Fundam Appl Toxicol 16, 337–47. [PubMed: 2055364]

DeAngelo AB, Daniel FB, Most BM, and Olsen GR (1996). The carcinogenicity of dichloroacetic acid in the male Fischer 344 rat. Toxicology 114, 207–21. [PubMed: 8980710]

DeAngelo AB, George MH, and House DE (1999). Hepatocarcinogenicity in the male B6C3F1 mouse following a lifetime exposure to dichloroacetic acid in the drinking water: dose-response determination and modes of action. J Toxicol Environ Health 58, 458–507.

De Preter G, Neveu MA, Danhier P, Brisson L, Payen VL, Porporato PE, Jordan BF, Sonveaux P, and Gallez B (2016). Inhibition of the pentose phosphate pathway by dichloroacetate unravels a missing link between aerobic glycolysis and cancer cell proliferation. Oncotarget 7, 2910–20. [PubMed: 26543237]

Eldridge SR, Butterworth BE, and Goldsworthy T (1993). Proliferating cell nuclear antigen: A marker of hepatocellular proliferation in rodents. Environ Health Perspect 101(suppl 5), 211–8. [PubMed: 7912188]

Eldridge SR, and Goldsworthy SM (1996). Cell proliferation rates in common cancer target tissues of B6C3F1 mice and F344 rats: effects of age, gender, and choice of marker. Fundam Appl Toxicol 32, 159–67. [PubMed: 8921319]

EPA. (2003). Toxicological review of dichloroacetic acid in support of summary information on Integrated Risk Information System (IRIS). National Center for Environmental Assessment, Washington, D.C. EPA/635/R-03/007. Available at: https://cfpub.epa.gov/ncea/iris/iris_documents/documents/toxreviews/0654tr.pdf (10 May 2017, date last accessed).

EPA. (2005a). Supplemental Guidance for Assessing Susceptibility from Early- Life Exposure to Carcinogens*, EPA/630/R-03/003F*. Risk Assessment Forum, Washington, DC http://www.epa.gov/ttnatw01/childrens_supplement_final.pdf (10 May 2017, date last accessed).

EPA. (2005b). *Guidelines for carcinogen risk assessment*. EPA/630/P-03/001F. Risk Assessment Forum, Washington, DC, 2005b Available at:https://www.epa.gov/sites/p 652 roduction/files/2013-09/documents/cancer_guidelines_final_3-25-05.pdf (10 May 2017, date last accessed).

Gatenby RA, and Gillies RJ (2004). Why do cancers have high aerobic glycolysis? Nat Rev Cancer 4, 891–9. [PubMed: 15516961]

Gavrieli Y, Sherman Y, and Ben-Sasson SA (1992). Identification of programmed cell death *in situ* via specific labeling of nuclear DNA fragmentation. J Cell Biol 119, 493–501. [PubMed: 1400587]

Ginsberg GL (2003). Assessing cancer risks from short-term exposures in children. Risk Anal 23, 19–34. [PubMed: 12635720]

Grandjean P, Barouki R, Bellinger DC, Casteleyn L, Chadwick LH, Cordier S, Etzel RA, Gray KA, Ha EH, Junien C, Karagas M, Kawamoto T, Paige Lawrence B, Perera FP, Halmes NC, Roberts SM, Tolson JK, and Portier CJ (2000). Reevaluating cancer risk estimates for short-term exposure scenarios. Toxicol Sci 58, 32–42. [PubMed: 11053538]

Hanahan D, and Weinberg RA (2011). Hallmarks of cancer: the next generation. Cell 144, 646–74. [PubMed: 21376230]

Herren-Freund SL, Pereira MA, Khoury MD, and Olson G (1987). The carcinogenicity of trichloroethylene and its metabolites, trichloroacetic acid and dichloroacetic acid, in mouse liver. Toxicol Appl Pharmacol 90, 183–9. [PubMed: 3629594]

Hester SD, Bhat V, Chorley BN, Carswell G, Jones W, Wehmas LC, and Wood CE (2016). Dose-Response Analysis of RNA-Seq Profiles in Archival Formalin-Fixed Paraffin-Embedded (FFPE) Samples. Toxicol Sci 154, 202–13. [PubMed: 27562560]

Holsapple MP, Pitot HC, Cohen SM, Boobis AR, Klaunig JE, Pastoor T, Dellarco VL, and Dragan YP (2006). Mode of action in relevance of rodent liver tumors to human cancer risk. Toxicol Sci 89, 51–6. [PubMed: 16221960]

Hoover RN, Hyer M, Pfeiffer RM, Adam E, Bond B, Cheville AL, Colton T, Hartge P, Hatch EE, Herbst AL, Karlan BY, Kaufman R, Noller KL, Palmer JR, Robboy SJ, Saal RC, Strohsnitter W,

Titus-Ernstoff L, and Troisi R (2011). Adverse health outcomes in women exposed *in utero* to diethylstilbestrol. N Engl J Med 365, 1304–14. [PubMed: 21991952]

IARC. (2004). Some Drinking Water Disinfectants and Contaminants, including arsenic: Dichloracetic Acid. IARC Monographs on the Evaluation of Carcinogenic Risks to Humans 84, 359–402.

Kato-Weinstein J, Lingohr MK, Orner GA, Thrall BD, and Bull RJ (1998). Effects of dichloroacetate on glycogen metabolism in B6C3F1 mice. Toxicology 130, 141–54. [PubMed: 9865481]

Kempa S, Itskovitz-Eldor J, Meshorer E, Aberdam D, and Nahmias Y (2015). Glycolysis-mediated changes in acetyl-CoA and histone acetylation control the early differentiation of embryonic stem cells. Cell Metab 21, 392–402. [PubMed: 25738455]

Kuppusamy SP, Kaiser JP, and Wesselkamper SC (2015). Epigenetic Regulation in Environmental Chemical Carcinogenesis and its Applicability in Human Health Risk Assessment. Int J Toxicol 34, 384–92. [PubMed: 26268770]

Leavitt SA, DeAngelo AB, George MH, and Ross JA (1997). Assessment of the mutagenicity of dichloroacetic acid in lacI transgenic B6C3F1 mouse liver. Carcinogenesis 18, 2101–6. [PubMed: 9395208]

Li B, and Dewey CN (2011). RSEM: accurate transcript quantification from RNA-Seq data with or without a reference genome. BMC Bioinformatics 12, 323. [PubMed: 21816040]

Lillycrop K, Myatt L, States JC, Thayer KA, Waalkes MP, and Rogers JM (2012). Predicting later-life outcomes of early-life exposures. Environ Health Perspect 120, 1353–61. [PubMed: 22672778]

Lingohr MK, Bull RJ, Kato-Weinstein J, and Thrall BD (2002). Dichloroacetate stimulates glycogen accumulation in primary hepatocytes through an insulin-independent mechanism. Toxicol Sci 68, 508–15. [PubMed: 12151648]

Mahabir S, Aagaard K, Anderson LM, Herceg Z, Hiatt RA, Hoover RN, Linet MS, Medina D, Potischman N, Tretli S, Trichopoulos D, Troisi R (2012). Challenges and opportunities in research on early-life events/exposures and cancer development later in life. Cancer Causes Control 23, 983–90. [PubMed: 22527169]

Moussaieff A, Rouleau M, Kitsberg D, Cohen M, Levy G, Barasch D, Nemirovski A, Shen-Orr S, Laevsky I, Amit M, Bomze D, Elena-Herrmann B, Scherf T, Nissim-Rafinia M, Pfaffl MW (2001). A new mathematical model for relative quantification in real-time RT709 PCR. Nucleic Acids Res 29, e45. [PubMed: 11328886]

Phan LM, Yeung SC, and Lee MH (2014). Cancer metabolic reprogramming: importance, main features, and potentials for precise targeted anti-cancer therapies. Cancer Biol Med 11, 1–19. [PubMed: 24738035]

Prins GS, Puga A, Rosenfeld CS, Sherr DH, Sly PD, Suk W, Sun Q, Tbalducoppari J, van den Hazel P, Walker CL, and Heindel JJ (2015). Life-Long Implications of Developmental Exposure to Environmental Stressors: New Perspectives. Endocrinology 156, 3408–15. [PubMed: 26241067]

Sanchez IM, and Bull RJ (1990). Early induction of reparative hyperplasia in B6C3F1 mice treated with dichloroacetate and trichloroacetate. Toxicology 64, 33–46. [PubMed: 2219131]

Shyh-Chang N, and Daley GQ (2015). Metabolic switches linked to pluripotency and embryonic stem cell differentiation. Cell Metab 21, 349–50. [PubMed: 25738450]

Siegel RL, Miller KD, and Jemal A (2016). Cancer statistics, 2016. CA Cancer J Clin 66, 7–30. [PubMed: 26742998]

Smith AH, Marshall G, Yuan Y, Ferreccio C, Liaw J, von Ehrenstein O, Steinmaus C, Bates MN, and Selvin S (2006). Increased mortality from lung cancer and bronchiectasis in young adults after exposure to arsenic in utero and in early childhood. Environ Health Perspect 114, 1293–6. [PubMed: 16882542]

Snyder RD, Pullman J, Carter JH, Carter HW, and DeAngelo AB (1995). In vivo administration of dichloroacetic acid suppresses spontaneous apoptosis in murine hepatocytes. Cancer Res 55, 3702–5. [PubMed: 7641179]

Stacpoole PW, Kurtz TL, Han Z, and Langaee T (2008). Role of dichloroacetate in the treatment of genetic mitochondrial diseases. Adv Drug Deliv Rev 60, 1478–87. [PubMed: 18647626]

Sutendra G, and Michelakis ED (2013). Pyruvate dehydrogenase kinase as a novel therapeutic target in oncology. Front Oncol 3, 38. [PubMed: 23471124]

Tzeng HF, Blackburn AC, Board PG, and Anders MW (2000). Polymorphism- and species-dependent inactivation of glutathione transferase zeta by dichloroacetate. Chem Res Toxicol 13, 231–6. [PubMed: 10775321]

Vandesompele J, De Preter K, Pattyn F, Poppe B, Van Roy N, De Paepe A, and Speleman F (2002). Accurate normalization of real-time quantitative RT-PCR data by geometric averaging of multiple internal control genes. Genome Biol 3, 1–12.

Vander Heiden MG, Cantley LC, and Thompson CB (2009). Understanding the Warburg effect: the metabolic requirements of cell proliferation. Science 324, 1029–33. [PubMed: 19460998]

Weinhouse C, Anderson OS, Bergin IL, Vandenbergh DJ, Gyekis JP, Dingman MA, Yang J, and Dolinoy DC (2014). Dose-dependent incidence of hepatic tumors in adult mice following perinatal exposure to bisphenol A. Environ Health Perspect 122, 485–91. [PubMed: 24487385]

WHO. (2000). Disinfectants and Disinfectant By-products. International Programme on Chemical Safety, Environmental Health Criteria Monograph 216 Geneva, Switzerland, 2000 Available at: http://www.inchem.org/documents/ehc/ehc/ehc216.htm (10 May 2017, date last accessed).

Wood CE, Hester SD, Chorley BN, Carswell G, George MH, Ward W, Vallanat B, Ren H, Fisher A, Lake AD, Okerberg CV, Gaillard ET, Moore TM, and Deangelo AB (2015a). Latent carcinogenicity of early-life exposure to dichloroacetic acid in mice. Carcinogenesis 36, 782–91. [PubMed: 25913432]

Wood CE, Hukkanen RR, Sura R, Jacobson-Kram D, Nolte T, Odin M, and Cohen SM (2015b). Scientific and Regulatory Policy Committee (SRPC) Review: Interpretation and Use of Cell Proliferation Data in Cancer Risk Assessment. Toxicol Pathol 43, 760–75. [PubMed: 25903269]

Zhang SL, Hu X, Zhang W, and Tam KY (2016). Unexpected Discovery of Dichloroacetate Derived Adenosine Triphosphate Competitors Targeting Pyruvate Dehydrogenase Kinase To Inhibit Cancer Proliferation. J Med Chem 59, 3562–8. [PubMed: 27006991]

Zhang Y, and Yang JM (2013). Altered energy metabolism in cancer: a unique opportunity for therapeutic intervention. *Cancer Biol Ther* 14, 81–9. [PubMed: 23192270]

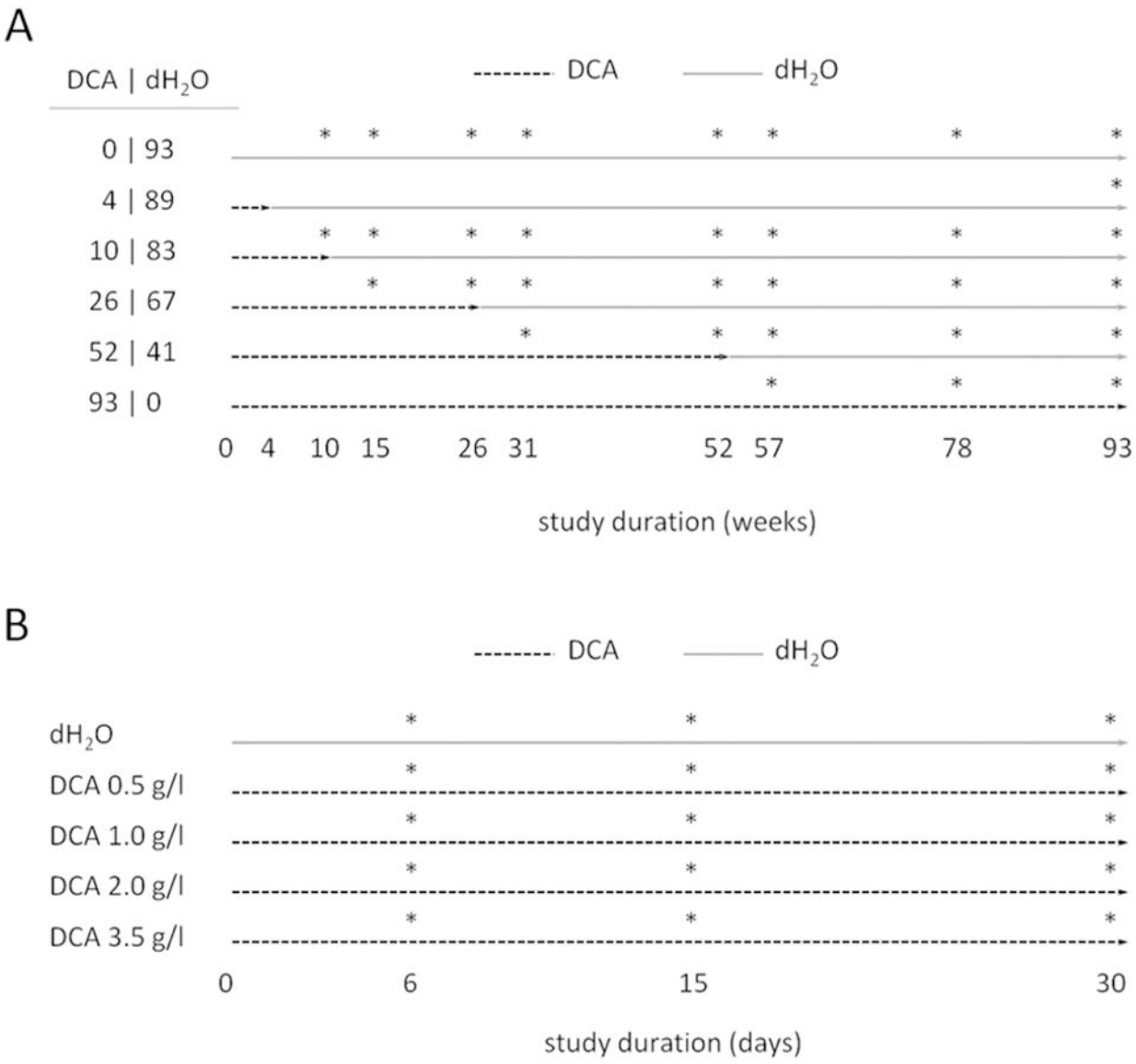

Figure 1.

Experimental design for the chronic stop-exposure (**A**) and short-term continuous exposure (**B**) studies of dichloroacetic acid (DCA) in male B6C3F1 mice. **A,** Treatments included deionized water (dH_2O, control); continuous DCA at 3.5 g/l in the drinking water; or 3.5 g/l DCA for 4, 10, 26, or 52 weeks followed by control dH_2O for up to 93 weeks. Broken arrows indicate DCA administration, solid arrows indicate dH2O, and asterisks (*) indicate time points of sampling for histopathology. Groups are designated by DCA and dH2O treatment times separated by a vertical bar. **B,** Treatments included dH_2O control or 0.5, 1.0, 2.0, and 3.5 g/l DCA in the drinking water for up to 30 days. Broken arrows indicate DCA administration, solid arrows indicate dH_2O, and asterisks (*) indicate interim and final time points. Mice were 4 weeks of age at the start of both experiments.

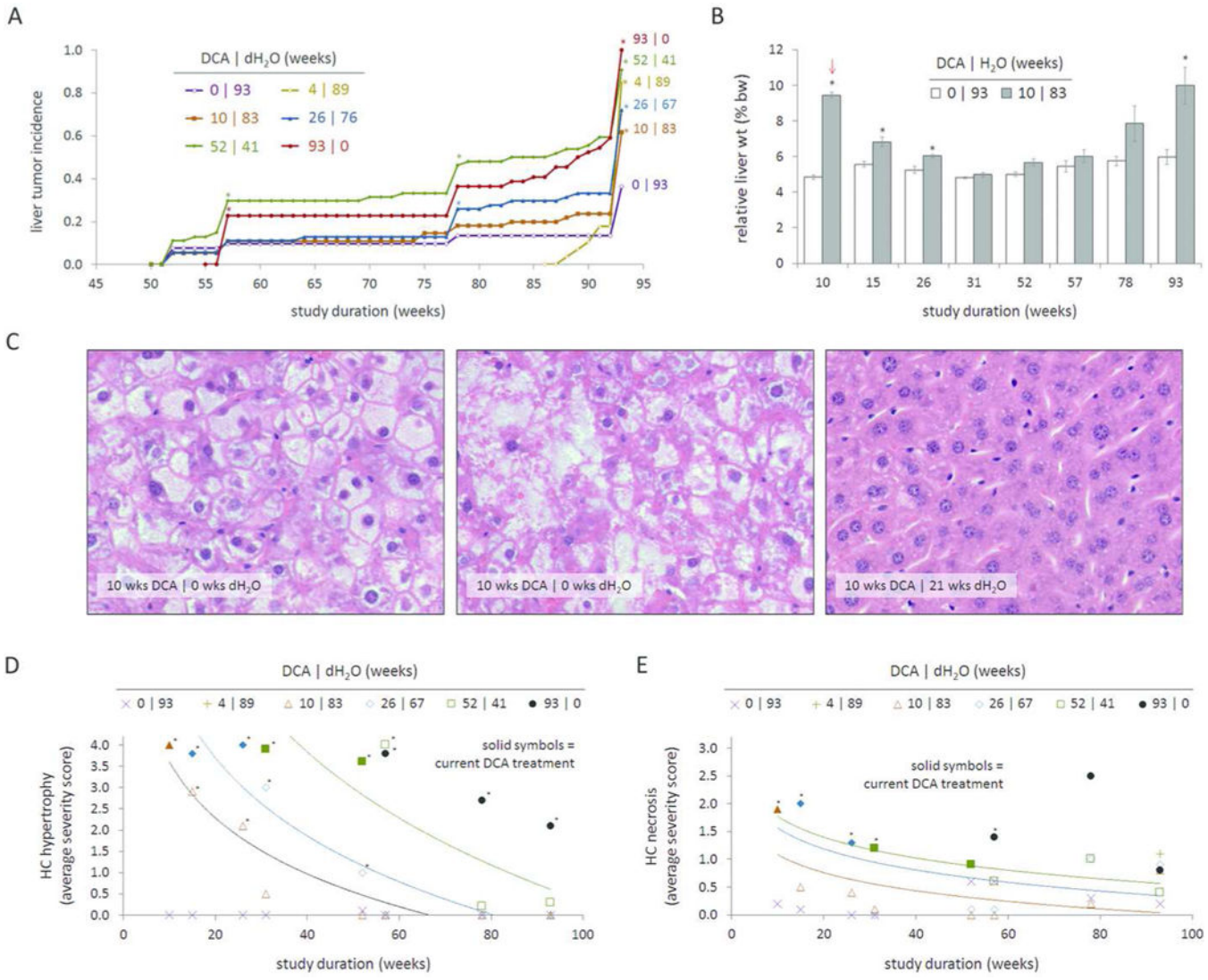

Figure 2.

Time course effects of early-life DCA treatment on liver pathology. **A,** Incidence of hepatocellular (HC) adenoma or carcinoma over time. Asterisks (*) indicate a significantly greater incidence at $P < 0.05$ compared to concurrent dH_2O control group. **B,** Relative liver weight in dH_2O (white bars) and 10-week DCA (dark bars) groups over time. Arrow indicates stoppage of DCA treatment. Asterisks (*) indicate adjusted $P < 0.05$ compared to concurrent dH_2O control group. **C,** Images showing marked HC hypertrophy with cytoplasmic vacuolation (left) and necrosis (middle) after 10 weeks of DCA treatment compared to normal liver at 31 weeks from the same 10-week DCA group (right), showing complete reversal of morphologic changes. H&E stain, 40x objective magnification. **D, E,** Persistence of HC hypertrophy (**D**) and necrosis (**E**) following DCA exposure. Solid symbols indicate current DCA treatment. Asterisk (*) indicates adjusted $P < 0.05$ in incidence compared to concurrent dH_2O control group.

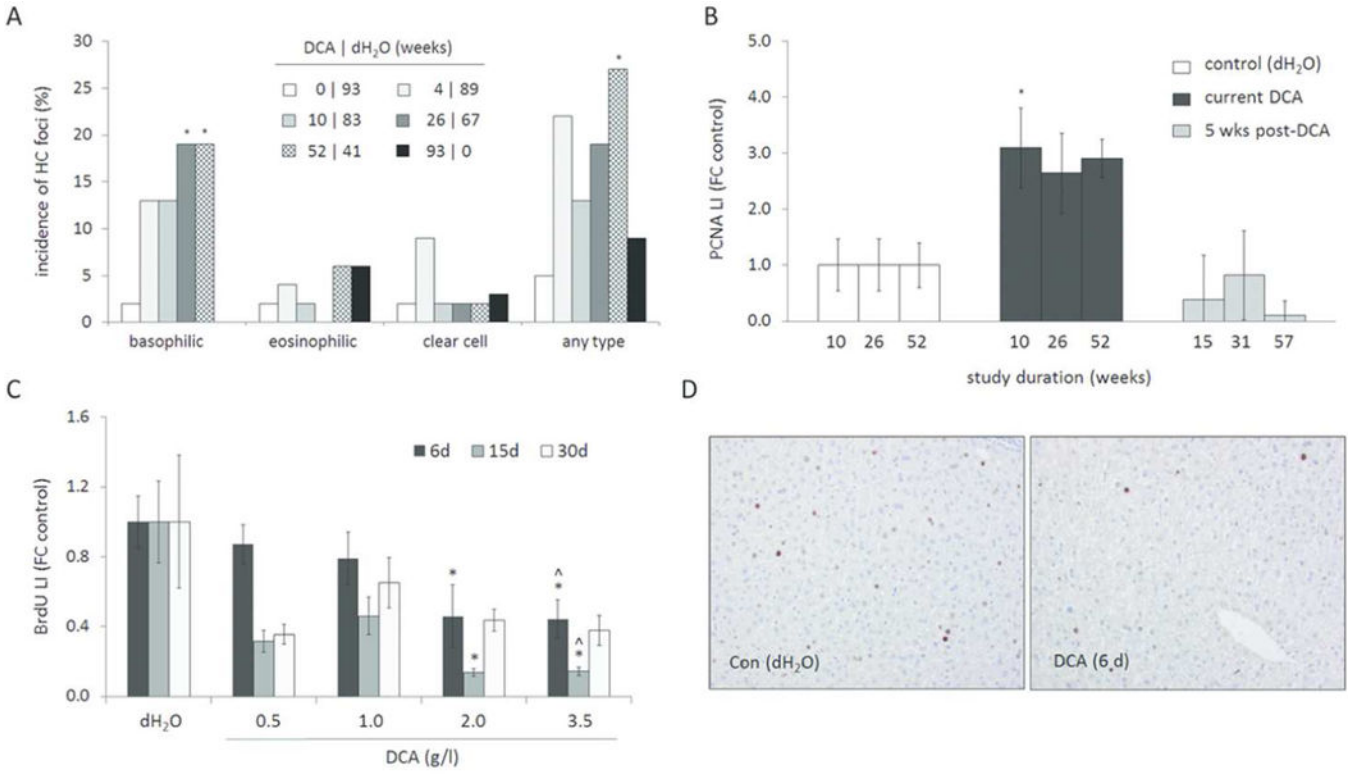

Figure 3.

Time course effects of DCA on liver cell proliferation in chronic and short-term studies. **A,** Cumulative incidence of proliferative (pre-neoplastic) hepatocellular foci in the chronic study at ≥31 weeks. Basophilic, eosinophilic, and clear cell indicate subtypes of foci; clear cell foci include “vacuolated” foci. Incidence data are provided in Supplementary Table S7. Note that the higher cumulative incidence in the 4-week DCA treatment group may be influenced by the lack of interim time points. **B,** Cell proliferation labeling index (LI) (%-positive cells) for current and prior DCA treatment in morphologically normal liver. **C,** Short-term dose effects of direct DCA exposure on liver cell proliferation LI determined by BrdU labeling index (%-positive cells). **D,** Representative images of BrdU labeling in liver sections from normal control and 3.5 g/l DCA groups at 6 days. Background staining with hematoxylin, 20x objective magnification. Full cell proliferation LI data sets are provided in Supplementary Tables S8 and S9. *adjusted $P < 0.05$ compared to Dh_2O Con group; ^ adjusted $P < 0.05$ for dose trend.

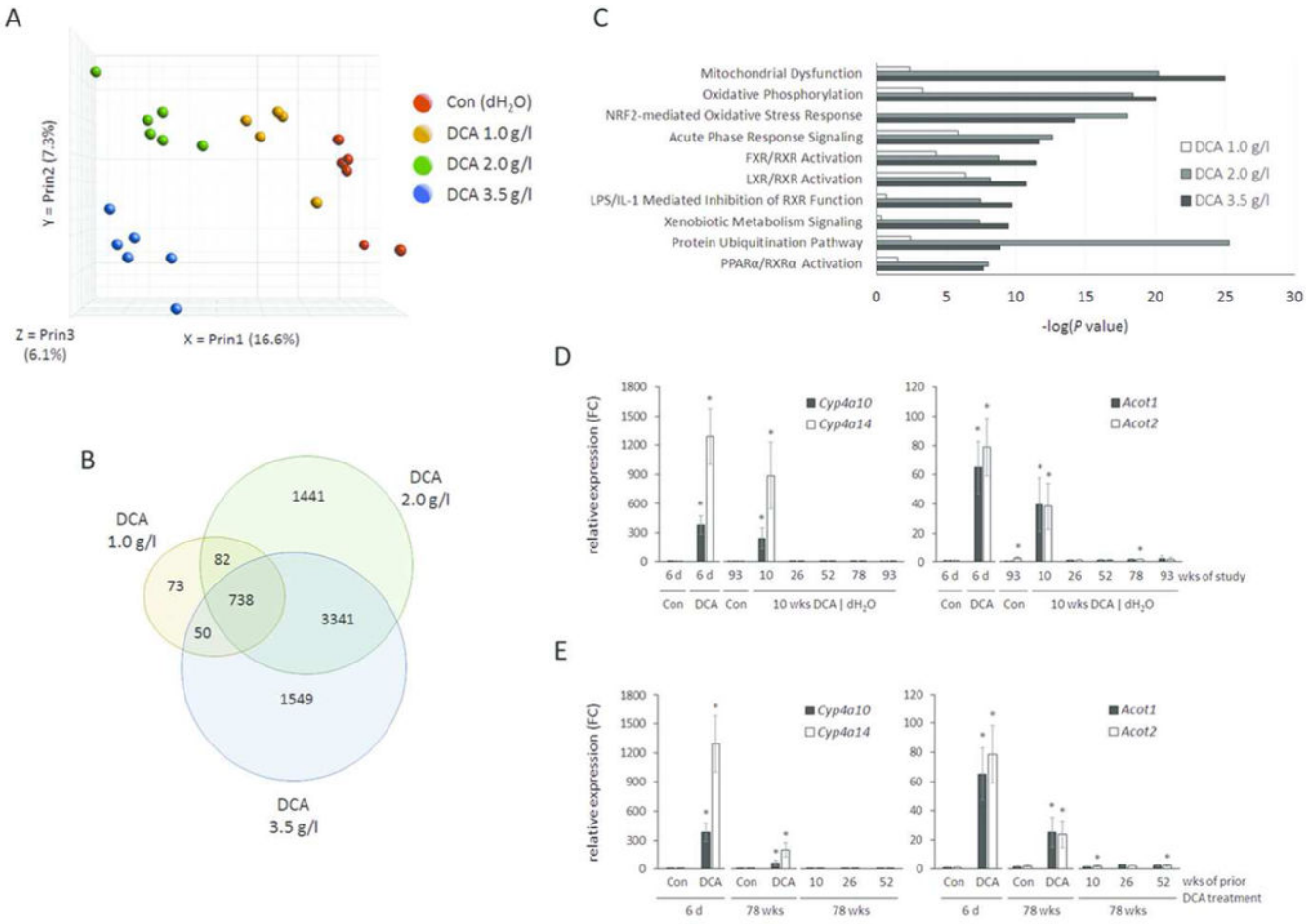

Figure 4.

Genomic effects of DCA following direct and prior exposure. **A–C**, RNA-seq profiles following treatment with 0, 1, 2 and 3.5 g/l DCA for 6 days. **A,** Principal component analysis of RPKM-normalized gene counts. Note clear separation of dose groups. **B,** Venn diagram showing overlap of significant DEGs for different DCA treatment groups with an FDR adjusted P value ≤ 0.05. Full DEG lists and RPKM-normalized counts are provided in Supplementary Table S11. **C,** Top canonical pathways in IPA shared across DCA treatment groups, ranked by -log(P value). A full list of canonical pathways is provided in Supplementary Table S12. **D, E,** Relative expression of select mRNA targets measured by RT qPCR. **D,** Time course effects following 10 weeks of DCA exposure. Bold labels on x-axis indicate week of study. **E,** Carry-over effects of prior DCA treatment at 78 weeks. Bold labels on x-axis indicate weeks of prior DCA exposure. Full RT-qPCR data sets are provided in Supplementary Table S15.

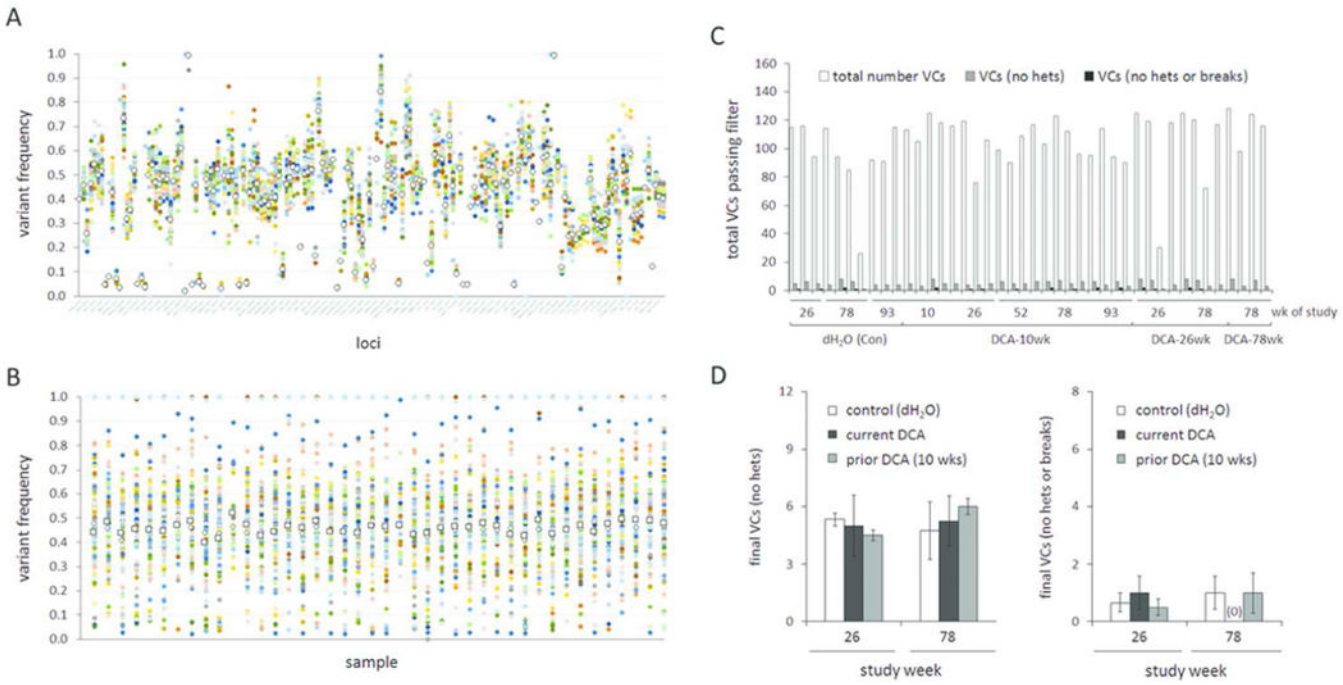

Figure 5.

Effects of current and prior treatment with DCA on DNA sequence variants in the liver. **A,** Frequency for each variant call (VC) at each locus as determined by DNA amplicon resequencing. Open circles represent mean frequency for each locus. **B,** Frequency of original quality-filtered VCs. Colored circles represent distinct VCs collated by sample. Open symbols represent mean variant frequency for each technical replicate (open diamonds and squares). **C,** Total number of variant calls in each sample (by group) presented as total (raw output, white bars), filtered for loci with parental heterozygosity (grey bars), and filtered for loci with parental heterozygosity and repeat breaks (black bars). **D,** Average number of variant calls (VCs) in dH2O control, prior DCA (10-week), and direct DCA groups at 26-week and 78-week time points. Left panel represents average VCs filtered by heterozygotes; right panel represents average VCs filtered by heterozygotes and breaks. Vertical bars indicate standard error of the mean. More detailed information is provided in Supplementary Table S16.

Table 1.

Latent effects of early-life exposure to DCA on the incidence of neoplastic lesions in the liver.

Duration of DCA exposure | control dH2O treatment (weeks)		**0 | 93**	**4 | 89**	**10 | 83**	**26 | 67**	**52 | 41**	**93 | 0**
No. Evaluated (<52 weeks)		**40**	**0**	**40**	**30**	**10**	**0**
None observed							
No. Evaluated (≥52 weeks)		**52**	**28**	**55**	**54**	**54**	**44**
Adenoma	No. indiv (%)	12 (23)	7 (25)	18 (33)	22 (41)	30 (56)*	26 (59)*
	No.indiv	0.3 ± 0.0	0.5 ± 0.1	0.4 ± 0.1	0.6 ± 0.1	1.0 ± 0.1	1.5 ± 0.2*
Carcinoma	No. indiv (%)	9 (17)	23 (82)*	27 (49)*	32 (59)*	35 (65)*	41 (93)*
	No./indiv	0.2 ± 0.0	1.3 ± 0.2*	0.8 ± 0.1*	1.3 ± 0.2*	1.2 ± 0.1*	2.5 ± 0.4*
Adenoma or	No. indiv (%)	19 (37)	24 (86)*	34 (62)*	39 (72)*	49 (91)*	44 (100)*
Carcinoma	No./indiv	0.5 ± 0.1	1.8 ± 0.3*	1.2 ± 0.2*	1.9 ± 0.3*	2.2 ± 0.3*	4.0 ± 0.4*

*(*)*Asterisk indicates significant difference (adjusted $P < 0.05$) compared to control group by one-sided Fisher's Exact Test. Counts include early death cases evaluated by histopathology. First hepatocellular tumor was observed at 52 weeks.